INTERNATIONAL JOURNAL OF AUTOMOTIVE AND MECHANICAL ENGINEERING (IJAME)
ISSN: 2229-8649 e-ISSN: 2180-1606
VOL. 17, ISSUE 2, 7890 – 7901
DOI: https://doi.org/10.15282/ijame.17.2.2020.08.0589

ORIGINAL ARTICLE

CFD Analysis of a Shell and Tube Heat Exchanger with Single Segmental Baffles

Shuvam Mohanty[1] and Rajesh Arora[2]

[1]School of Engineering and IT, UNSW Canberra@ADFA, 2612 Canberra, ACT, AUSTRALIA
[2]Department of Mechanical Engineering, Amity University, 122413 Gurgaon, Haryana, INDIA

ABSTRACT – In this investigation, a comprehensive approach is established in detail to analyse the effectiveness of the shell and tube heat exchanger (STE) with 50% baffle cuts (B_c) with varying number of baffles. CFD simulations were conducted on a single pass and single tube heat exchanger(HE) using water as working fluid. A counterflow technique is implemented for this simulation study. Based on different approaches made on design analysis for a heat exchanger, here, a mini shell and tube exchanger (STE) computational model is developed. Commercial CFD software package ANSYS-Fluent 14.0 was used for computational analysis and comparison with existing literature in the view of certain variables; in particular, baffle cut, baffle spacing, the outcome of shell and tube diameter on the pressure drop and heat transfer coefficient. However, the simulation results are more circumscribed with the applied turbulence models such as Spalart-Allmaras, k-ε standard and k-ε realizable. For determining the best among the turbulence models, the computational results are validated with the existing literature. The proposed study portrays an in-depth outlook and visualization of heat transfer coefficient and pressure drop along the length of the heat exchanger(HE). The modified design of the heat exchanger yields a maximum of 44% pressure drop reduction and an increment of 60.66% in heat transfer.

ARTICLE HISTORY
Revised:13th Feb 2020
Accepted: 17th Apr 2020

KEYWORDS
CFD, STE, ANSYS-Fluent, Spalart-Allmaras, k-ε standard and k-ε realisable, Baffle cut(B_c).

NOMENCLATURE

B	central baffle spacing (mm)	*Greek symbols*	
B_c	baffle cut (%)	ε	viscous dissipation rate (m^2/s^3)
$C_{1\varepsilon}$, $C_{2\varepsilon}$, $C_{3\varepsilon}$, C_l, C_2	constants of transport equations	k	closure coefficient of transport equations
C_{b1}, C_{b2}, C_{w1}, C_{w2}, C_{w3}, C_{v1}	closure coefficients of transport equations	λ	viscosity coefficient
f_{v1}, f_w	viscous damping function	μ	dynamic viscosity (Pa s)
G_b	generation of turbulence due to buoyancy	μ_t	turbulent viscosity (Pa s)
k	kinetic energy	υ	kinematic viscosity (m^2/s)
K	thermal conductivity (W/m-K)	ρ	density (kg/m^3)
N_b	number of baffles	σ_k	turbulent Prandtl numbers for k
N_t	number of tubes	σ_v	constant of transport equations
P	pressure (Pa)	σ_ε	turbulent Prandtl numbers for ε
V	velocity	Φ	dissipation function
S	scalar measure of the deformation tensor	*Abbreviations*	
$S\varepsilon$, Sv	user-defined source terms of transport equations	STE	shell and tube heat exchanger
u, v, w	velocity components (m/s)	HE	heat exchanger
x, y, z	position coordinates		

INTRODUCTION

For most productive industrial operations, STE's are widely chosen for better possible heat transfer, and many pieces of literature have provided evidence that by analytical and computational methods [1,11,26,27]. As far as the flow technique is concerned, the counterflow configuration is the preeminent among them for effective analysis suggested by Mohanty et al.[6]. The advantages in terms of compactness and design make shell tube heat exchangers more desirable for industrial purposes such as power generation, chemical industry, and thermal power industries. The Tubular Exchanger Manufacturers Association (TEMA) is an association that upholds or sets the standard for heat exchanger construction [28]. The heat exchanger is designed by making some vital correlations and an analytical based approach. The correlations can be obtained by altering the design specifications iteratively. For a particular iteration, the performance of the heat exchanger can be evaluated; if it seems to be unsatisfactory, then some design parameters were modified in the right direction. However, performing such type of task is time-consuming. It is straightforward to amend

*CORRESPONDING AUTHOR | Shuvam Mohanty | ✉ shuvammohanty724@gmail.com

the tube side parameters in the heat transfer operation. Still, it is very challenging to acquire the precise arrangement for the shell side during the heat transfer because, in the shell side, different leakage paths and bypass streams are present around the flow zone. Despite the fact of difficulty, CFD made it more straightforward in terms of flow field visualisation and temperature distribution by simplifying the assessment weakness.

Nowadays, for economical operation, numerical methods are extensively used to reduce the experimental cost and time, relatively. A small 3-D heat exchanger is designed in the present analysis, and due to the size, the leakages are negligible or don't exist in comparison to the main flow stream, even though the shell side geometry is complicated because of the baffles. Baffles are present in the heat exchanger for adequate circulation of working fluid inside the shell from inlet to outlet recommended by Trp et al., Gajapathy et al. [2,5]. The most conventional baffles, such as single segmental circular baffles, are used here for the simulation. The baffles have a cut in the middle, and those baffle cuts are inevitably essential for allowing the fluid to cross through the shell. The baffle cuts positions are not the same throughout the shell. The orientation was reformed (cut face down, cut face up) and is designed in such a way that leads to creating a flow path across the tube bundles. The baffle spacing is maintained to visualise the flow structure. The shell and tube configuration is as shown in Figure 1, and the flow structure is very much proportional to the baffle cuts and spacing inside the shell. Here the influence of baffle cuts and spacing over the heat transfer and pressure drop are analysed.

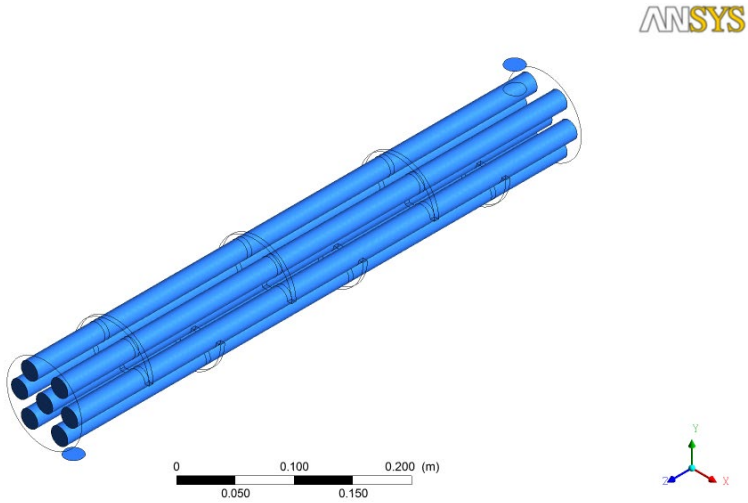

Figure 1. Shell and tube heat exchanger with six baffles.

Andrews and Master [1] performed a 3D CFD simulation of a helical tube heat exchanger with three different helix angles, i.e., 10°, 25°, and 40° concerning the radial axis. The study concentration is on the recirculation zones, back mixing in the inner and outer regions of the shell. Trp et al. [2] have studied a phenomenon for transient heat transfer of 2-D STE within a control volume using commercial CFD software ANSYS. Developing codes in FORTRAN and imposing boundary conditions at the inlet and outlet of heat exchanger (HE), the model was validated with some experimental results. Investigation of tube side heat transfer has explored by Karno and Ajib [3] on an STE. The effect of longitudinal as well as transverse tube pitch in the inline and staggered tube arrangements was simulated for inspection of different thermodynamic properties such as heat transfer coefficients, Nusselt number, and thermal performance. Enhancement of heat transfer was reported in a helical double pipe heat exchanger using CFD fluent package 6.2 by Jayakumar et al. [4]. Heat transfer was analysed considering different properties, methodology and was validated in contrast with a fabricated experimental setup. Some commercially available CFD codes PHOENICS were used by Gajapathy et al. [5] for thermo-hydraulic research of a transitional heat exchanger in a pool-type liquid metal. Using those codes prediction of temperature distribution in the tube side and shell side has obtained with or without provision of flow devices.

Under turbulent flow conditions, the thermo-fluid analysis was carried out by Mandal and Nigam [7] in a helical tube heat exchanger. Concurrent interaction between water and hot gas taken place inside the heat exchanger. For this fluid to fluid interaction, Reynolds number, Nusselt number and friction factor were considered in their literature for computational analysis. A correlation-based approach has made by Kharat et al. [8] for the discrepancies of gaps in the coils and tubes of a heat exchanger. Mathematical models were developed for CFD analysis, and simulated values were compared with the experimental results. This investigation shows around 3-4% error in the CFD calculation. An ideal approach of reducing the baffle cut up to 36% and 25% by Ozden and Tari [9] on a small lab-scale model for STE has been simulated for better visualisation of the flow structure interaction, backflow, pressure drop inside the shell. Following that few researchers like Chen et al. [10], Jadhav and Koli [11] also investigated the STE with numerical simulation.

A comprehensive simulation approach was made by Jayakumar et al. [12] on the helically coiled heat exchanger. Subsequently, Pandey and Nema [13] and Mandal et al. [14] considering two-phase fluid flow approach because single-phase became trivial then for simulation. However, numerical simulation implies a much better insight into the real world heat transfer analysis. Convective heat transfer at different particle sizes was examined by various researchers [14-16] in the developing regions of the tube by introducing the CFD method. A passive technique of using a twisted tube was

addressed [17-19] to compare with plane tubes. At present, the twisted tube has limited application in comparison with straight passages for heat transfer analysis. To study the pressure field, temperature field and path lines, Yang and Liu [20] have numerically investigated the shell and tube heat exchanger utilising rod baffles.

Moreover, the aim is to generalise between the plate baffle heat exchanger and rod baffle heat exchanger using Fluent 6.3 and Gambit 2.3. Pal et al. [21] have found the huge advantages of STE, which made it the most convenient type of heat exchanger for industrial purpose. An attempt was made to investigate the thermodynamics of small shell and tube heat exchanger using with and without baffles in the open FOAM with the help of CFD codes. For small heat exchanges nozzle region has some substantial role for the heat transfer and k-ε turbulence model emerges to be the best among the other profound models because the boundary conditions seem to be realistic. Baffle selection and thermo-hydraulic performance were addressed by El Maakoul et al. [22] for an STHX using ANSYS Fluent. Different parameters such as flow distribution of shell side, heat transfer coefficient, and pressure drop were disclosed in that paper with low flow rates using a single segmental baffle.

Major factors for a shell and tube heat exchanger were evaluated by Bichkar et al. [23] using different baffles orientation such as single segmental, double segmental and helical baffles. Single segmental baffles form a dead zone inside, where no heat transfer was taking place while double segmental framing out to be better. Double segmental baffles smartly minimise the vibrational effect. A CFD analysis made by Nada et al. [24] on heat transfer characteristics for a helically coiled heat exchanger introduced. Correlations based approach was made for analysing Nusselt number and Reynolds number. To reduce the capital and to operate cost for the STE Shinde and Chavan [25] have introduced new baffle materials, e.g., FRP in recent years with different helix angles. Among different helix angles, larger helix angles show lower pressure drop and heat transfer, but the smaller lower angles bring higher heat transfer and pressure drops.

In real practice, both the effectiveness and pressure drop are directly proportional to the fluid flow path, baffle spacing inside the shell. Hence more the complexity of baffles inside the shell the transfer of heat will be more; however, the pressure drop increases in addition to the consumption of higher pumping power are required. So the effort made to minimise the pressure drop inside the shell side of the heat exchanger implementing different numbers of continuous baffles and baffle cuts (alternate positions) is introduced on a small scale. The implementation of a 25% baffle cut is widespread in STE, but a 50% baffle cut for STE was not effectively analysed. For this present analysis, the baffle cuts have increased to 50% without changing the angle of inclination. For the design simplification, the edge of those single segmental baffles is kept as 90º. ANSYS Fluent version 14.0 is used for mesh generation because simulation results are sensitive to the meshing. After choosing adequate mesh, discretisation method, and viscous model, the simulation is performed with three different fluid flow rates altering the number of baffles, baffle spacing and baffle cuts. Different thermal properties are calculated for the shell side and later compared these results with existing computational literature [9] for the numerical simulation.

MODELLING DETAILS

The CFD simulation study was performed on a small lab-scale model of STE for accurate visualisation of transfer of heat and pressure drop for shell side analysis of the heat exchanger. Numerous geometric parameters and design parameters were included for modelling of the heat exchanger. The information regarding modelling parameters is stated in Table 1. The geometric model prepared in the ANSYS shown in Figure 1 for six baffles with a 50% baffle cut. A 50% baffle cut is introduced, which is halfway in line with tubes of the central row. Water is used as the working fluid, and aluminium is chosen for the material of construction.

Governing Equation

To characterise the laws of conservation of mass, momentum, and energy for an incompressible fluid and the heat transfer inside the heat exchanger are described below.

Conservation of mass:

$$\nabla.(\rho V)=0 \tag{1}$$

Momentum equation:

In x-direction;
$$\nabla.(\rho uV)= -\frac{\partial \rho}{\partial x}+\frac{\partial \tau_{xx}}{\partial x}+\frac{\partial \tau_{yx}}{\partial y}+\frac{\partial \tau_{zx}}{\partial z} \tag{2}$$

In y-direction;
$$\nabla.(\rho \upsilon V)= -\frac{\partial \rho}{\partial y}+\frac{\partial \tau_{xy}}{\partial x}+\frac{\partial \tau_{yy}}{\partial y}+\frac{\partial \tau_{zy}}{\partial z}+\rho g \tag{3}$$

In z-direction;
$$\nabla.(\rho wV)= -\frac{\partial \rho}{\partial z}+\frac{\partial \tau_{xz}}{\partial x}+\frac{\partial \tau_{yz}}{\partial y}+\frac{\partial \tau_{zz}}{\partial z} \tag{4}$$

Energy equation:

$$\nabla.(\rho eV)= -p\nabla.V+\nabla.(k\nabla T)+q+\varphi \tag{5}$$

φ is the heat dissipation calculated from;

$$\varphi = \mu\left[2\left[\left(\frac{\partial u}{\partial x}\right)^2 + \left(\frac{\partial v}{\partial y}\right)^2 + \left(\frac{\partial w}{\partial z}\right)^2\right]\right] + \left(\frac{\partial u}{\partial y} + \frac{\partial v}{\partial x}\right)^2 + \left(\frac{\partial u}{\partial z} + \frac{\partial v}{\partial x}\right)^2 + \left(\frac{\partial v}{\partial z} + \frac{\partial w}{\partial y}\right)^2 + \lambda(\nabla . V)^2 \quad (6)$$

Geometrical consideration

For this small-scale model of STE, the crucial boundary condition has to be temperature and fluid flow rate at the inlet. For obtaining higher heat transfer at the expense of low-pressure drop at the outlet of shell and tube, the desired boundary condition is implemented in terms of fluid flow rate and temperature. The details of geometrical parameters are listed below in Table 1. No-slip condition is assigned at the surface, and gravity is assigned to the Y-axis. The tubes and shells are made solid with inlet temperatures at 450 K and 300 K, respectively.

Table 1. Geometrical parameters.

Shell diameter, D_s	90 mm
Diameter of tube, D_t	20 mm
Tubes, N_t	7
Length of HE, L	600 mm
Inlet temperature for shell side, T_s	300 K
Tube inlet temperature, T_t	450 K
Baffle cut, B_c	50%
Number of baffles, N_b	6
Baffle spacing, B	85.7 mm

Mesh generation

Meshing is performed in the ANSYS meshing software, and two different types of mesh sizes are selected, i.e., coarse and fine with 870,988 elements and 1,536,345 elements, respectively, as in Table 2. For this present investigation, the simulation runs on a progressively finer grid by changing the local refinements to check the variation of computational parameters. It is evident from Figure 2 that applying fine and coarse mesh size, the results are found to be in good agreement with the actual results. However, medium mesh size results are also good, but for the comparison purpose, both coarse and fine mesh are taken into consideration. So considering the solution accuracy and computation time, the grids are chosen. The tetrahedral mesh is selected for surface meshing, which is shown in Figure 3..

Table 2. Number of cells in a different type of mesh.

Size of mesh	Elements	Nodes
Coarse	870,988	174071
Medium	1,156,564	231144
Fine	1,536,345	307043

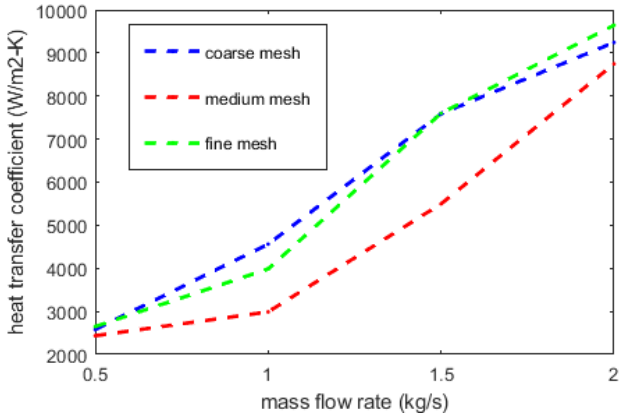

Figure 2. Grid independence test.

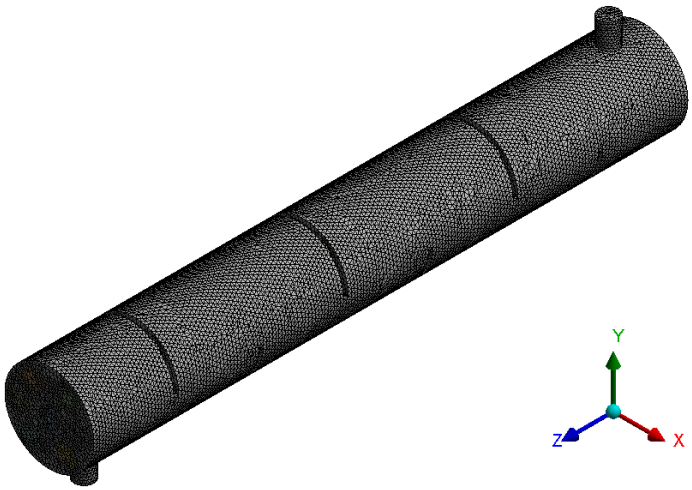

Figure 3. Grid structure of the computational domain.

Turbulence modelling

As the flow is not laminar inside the heat exchanger, the transient simulation is chosen for the simulation, and there are few standard norms based on which turbulence models should be selected. That's why different turbulence models must be selected for separate studies. In this study, three different types of turbulent models are addressed, such as Spalart-Allmaras, k-ε standard and k-ε realisable. The Spalart-Allmaras model is based on kinematic eddy viscosity and mixing length. This mixing length defines the transport of the turbulent viscosity. This is a robust model, fast to implement when modelling a specialised flow and solves only one transport equation, i.e., turbulent viscosity. In flows where convection and diffusion cause significant differences between production and destruction of turbulence, then the k-ε model comes into consideration. So, considering the dynamics of the turbulence k-ε model introduced, which focuses on the mechanism that affects the turbulent kinetic energy. On the other hand, two k-ε models, i.e., standard and realisable, are seems to be the most crucial for shell and tube analysis.

The Spalart-Allmaras turbulence equation stated below with closure functions and coefficient. The equations for the simulation analysis are mentioned below;

$$\frac{\partial}{\partial x_i}(\rho v u_i) = \rho v C_{b1} S - C_{w1} f_w \rho \left(\frac{V}{d}\right)^2 + \frac{1}{\sigma_v}\left[\frac{\partial}{\partial x_j}\left\{(v\rho + \mu)\frac{\partial V}{\partial x_j}\right\} + C_{b2}\rho\left(\frac{\partial V}{\partial x_j}\right)^2\right] + S_v \tag{7}$$

$$\mu_t = \rho f_{v1} v \tag{8}$$

$$\mathrm{C}_{b1} = 0.1355, \mathrm{C}_{b2} = 0.622, \mathrm{C}_{v1} = 7.1,\ \sigma_v = 0.667, \mathrm{C}_{w2} = 0.3, \mathrm{C}_{w3} = 2, k = 0.85$$

The standard k-ε model only valid for turbulent and non-separated flow, and it solves both turbulent kinetic energy and rate of dissipation of kinetic energy. It also offers good convergence; that's why it framed as a general-purpose model, whereas k-ε realisable improves the performance of complex geometries, and it resolves boundary layers by two-equation models.

$$\mathrm{C}_{b1} = 0.09, \mathrm{C}_{b2} = 1.44, \mathrm{C}_{v1} = 1.92,\ \sigma_v = 1, \mathrm{C}_{w2} = 1.3, \mathrm{C}_{w3} = 0.85, k = 0.85$$

The k-ε realisable model equation is as follows;

$$\frac{\partial}{\partial x_j}(\rho\varepsilon u_j) = \frac{\partial}{\partial x_j}\left[\left(\mu + \frac{\mu_t}{\sigma_\varepsilon}\right)\frac{\partial \varepsilon}{\partial x_j}\right] + \rho \mathrm{C}_1 S\varepsilon + \mathrm{C}_{1\varepsilon}\frac{\varepsilon}{k}\mathrm{C}_{3\varepsilon}G_b - \mathrm{C}_2\rho\frac{\varepsilon^2}{k + \sqrt{\varepsilon v}} + S_v \tag{9}$$

$$\mathrm{C}_{2\varepsilon} = 1.9, \sigma_k = 1, \sigma_\varepsilon = 1.2$$

After the turbulence models, the discretisation plays an important role. Here the SIMPLE algorithm is chosen for calculating the pressure and velocities. The momentum equations calculation needs to be done sequentially. In the SIMPLE algorithm, an initial guess is made for pressure and velocity component to discretise the momentum equation. In the second step, it solves the pressure correction equation. After correcting the pressure and velocities, the algorithm jumps to resolve all other discretised transport equations. If the simulation reaches the convergence, then it will stop otherwise, one more iteration will be follow up.

For the heat exchanger analysis, both first and second-order discretisation scheme is implemented, alternatively. Both first and second-order discretisation is carefully chosen for kinetic energy, momentum, and dissipation rate. Choosing 1st

order discretisation provides an advantage of better convergence as compared to the 2nd order, whereas second-order discretisation reduces the discretisation error.

DISCUSSION OF RESULTS

For comparison and validation of this present CFD model, the existing CFD simulation study [9] has chosen with different baffles. Different output parameters such as pressure drop, heat transfer coefficient, and total heat transfer are analysed by altering the design parameters such as the number of baffles, baffle cuts (b_c) and baffle spacing — the portrayal of computational simulation consequences as described in Table 3.

Table 3 displays all the obtained output parameters after the CFD simulation. The outlet temperature, pressure drop, and heat transfer rate are directly found after the computational simulation. However, the heat transfer coefficients are calculated using the LMTD method from the change in temperature and heat transfer area. From the above Table 3, it illustrates that cases A, B, C, D results are not convenient because there is an increase in temperature outlet by increasing the fluid flow rate for the same heat exchanger area. It violates the principle, as the flow becomes faster, the heat exchanger liquids don't get enough time to interact with each other. However, for the rest of the cases, the simulated results are satisfactory, as the temperature increases only by decreasing the fluid flow rate. Hence considering the difference, the heat transfer results are reasonable. Among those cases, k-ε standard and k-ε realisable 1st order discretisation are providing the best results, but the case-I results seem to be unsatisfactory. Because in case-I, there is an unpredictable heat transfer rise taking place which practically not possible to achieve.

Table 3. Computational investigation using different viscous models and discretisation methods.

Case	Turbulence model	Grids	Mass flow rate (kg/s)	Result of CFD Analysis			
				Shell side outlet temperature (K)	Heat transfer coefficient (W/m^2 K)	Pressure drop at Shell side (Pa)	Total heat transfer (W)
A	k-ε standard	Coarse (870,988)	0.5	325.86	1847.22	2138.53	115818.69
			1	328.77	2777.75	8664.20	179106.58
			2	330.23	5422.60	35859.37	231598.42
B	k-ε standard 2nd order	Coarse (870,988)	0.5	327.39	2577.58	2602.60	166280.64
			1	329.02	4560.94	8139.22	208642.3
			2	331.47	9244.75	41464.54	201263.31
C	k-ε realizable	Coarse (870,988)	0.5	325.67	1518.68	2261.13	196407.8
			1	322.98	3133.57	9079.50	173538.14
			2	321.34	6051.13	36394.83	155568.83
D	Spalart–Allmaras	Fine (1,536,345)	0.5	317.69	2412.99	2097.57	81630.64
			1	320.13	3613.29	9035.14	92956.22
			2	321.46	3484.67	2412.99	97382.38
E	Spalart–Allmaras 2nd order	Fine (1,536,345)	0.5	317.79	2412.99	2642.97	82068.35
			1	309.56	3962.02	10671.7	872633.94
			2	305.01	6241.22	39254.78	315441.31
F	k-ε standard	Fine (1,536,345)	0.5	344.98	2996.73	2103.10	70578.21
			1	340.96	5168.67	5420.29	149842.63
			2	335.54	9638.84	23182.95	251988.43
G	k-ε standard 2nd order	Fine (1,536,345)	0.5	348.36	2646.3	2171.31	71909.02
			1	342.20	3984.58	5667.41	1838292
			2	338.57	9645.41	23950.62	32580.06
H	k-ε realizable	Fine (1,536,345)	0.5	341.34	2798.65	2104.20	180519.39
			1	337.81	4125.67	8643.02	165755.09
			2	324.33	7951.34	34625.79	109380.69
I	k-ε realizable 2nd order	Fine (1,536,345)	0.5	371.01	2651.88	2159.20	304634.72
			1	363.60	6124.59	10218.90	386551.03
			2	349.23	10569.67	31549.65	564327.89

Apart from that, the pressure drop is calculated for the heat exchanger, which shows there is a rise in pressure at the outlet by increasing the fluid flow rate. However, the drop is quite usual due to the baffles spacing and baffle cuts, which impede the motion of the fluid. After finding the adequate turbulence model, the heat exchanger with 8, 10, and 12 numbers of baffles are simulated. Simulation results are mentioned in Table 4, which explains that increasing the number the baffles increases the pressure drop and outlet temperature irrespective of baffle spacing. Hence the unexplored relation between the baffle spacing and heat exchanger geometry has shown in this study. Table 4 shows the optimum values for baffle spacing and shell diameter ratio.

Table 4. Relation between baffle spacing and design parameters.

Number of baffles, N_b	6	8	10	12
Central baffle spacing, B (mm)	85.7	66.67	54.54	46.15
Ratio of B/D_S	0.95	0.74	0.6	0.51

Table 5. Computational results for varying numbers of baffles, N_b.

N_b	Mass Flow rate (kg/s)	Computational results			
		Shell side outlet Temperature (K)	Heat transfer coeff. (W/m2 K)	Pressure drop at shell side (Pa)	Total heat transfer (W)
6	0.5	344.98	2996.73	1503.10	70578.21
	1	340.96	5168.67	5420.29	149842.63
	2	335.54	9638.84	23182.95	251988.43
8	0.5	345.14	2778.89	2178	196411.47
	1	342.68	5865	8514.23	234650.87
	2	338.97	9854.23	30987.02	426755.1
10	0.5	348.60	2971.16	2107.96	169062.98
	1	345.89	4698.31	9854.26	274988
	2	341.84	9125.65	38648.77	421896.54
12	0.5	357.92	3502	1882.94	249856.45
	1	352.13	5649.94	10975.61	356211.79
	2	347.64	10624.83	45698.52	512697.02

In Table 6, the 50% baffle cut CFD simulation results are compared with 36% baffle cut simulations. It shows the percentage difference between these calculations.

Table 6. Percentage difference between Bc=36% and Bc=50%.

N_b	Mass flow rate (kg/s)	Heat transfer coefficient (W/m^2 K) in %	Pressure drop at shell side (Pa) in %	Total heat transfer (W) in %
6	0.5	16.1	-1.25	20.22
	1	9.87	-13.79	12.05
	2	29.78	-7.67	4.55
8	0.5	2.87	-1.28	54.32
	1	27.2	-1.4	37.98
	2	20.73	-10.92	36.97
10	0.5	3.43	-44.31	44.3
	1	5.24	-21.20	41.95
	2	3.74	-22.10	29.2
12	0.5	13.9	-38.05	60.66
	1	9.46	-40.62	52.08
	2	9.44	-33.33	36.91

The comparison illustrated in Table 5 shows there is an increase in heat transfer by increasing the number of baffles favourably with a lower mass flow rate. On the other hand, there is a decrease in pressure at a lower flow rate and a 50% baffle cut in contrast with the 36% baffle cut. However, the pressure drop is directly related to the ratio of baffle spacing to shell diameter. The simulation result predicts the optimum B/D_s ratio for the heat exchanger analysis should have lies in between 0.3 to 0.6. The velocity flow paths for varying numbers of baffles are shown below.

Effect of Baffle Cut (B_c) on Heat Transfer and Pressure Drop

Changing the number of baffles and baffle spacing the effect of pressure drop and total heat transfer on STE is investigated. The 50% baffle cut provides better results in contrast with the 36% baffle cut. After increasing the number of baffles, the baffle spacing will decrease for a fixed heat exchanger length. For every CFD investigation, the simulation has to follow the same cycle. The new geometry after increasing the number of baffles is re-meshed in ANSYS and then follows the same track for simulation. By decreasing the baffle spacing, the heat transfer increases simultaneously as well as the pressure drop. The pressure drop values increase due to an increase in fluid flow, but it is lower in comparison with the 36% baffle cut. That's why the 50% baffle cut results improve the performance of the heat exchanger, and it has shown already in terms of percentage difference. For 6, 8 and 10 baffles, the percentage difference is less for lower mass flow rate.

In Figure 4, the velocity streamlines are shown for varying numbers of baffles at 0.5 kg/s mass flow rate. From Figure 5, it can be observed that the liquid water after hitting the baffle plates changes its direction so that the crossflow inside the heat exchanger is not effectively possible. However, for 10 and 12 numbers of baffles, there is a recirculation zone visualised briefly in Figure 5(c) and 5(d) which implies the flow is well developed, and recirculation is possible. These simulations express 10, and 12 number of baffles hold better acceptable design for this heat exchanger. Moreover, in comparison with the 36% baffle cut the 50% baffle cut gives better performance in terms of higher heat transfer and lower pressure drop.

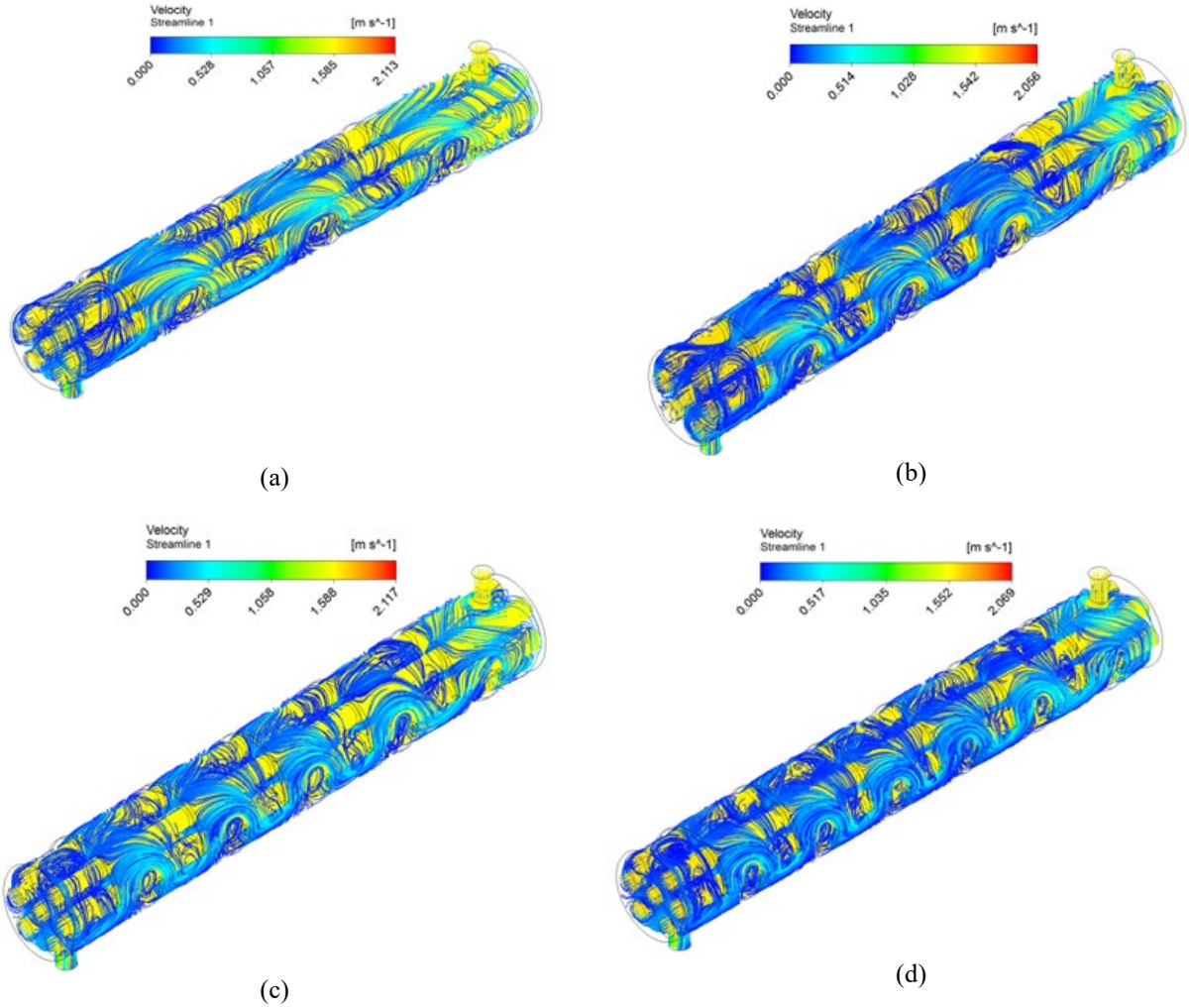

Figure 4. Velocity profile for (a) N_b=6, (b) N_b=8, (c) N_b=10, (d) N_b=12.

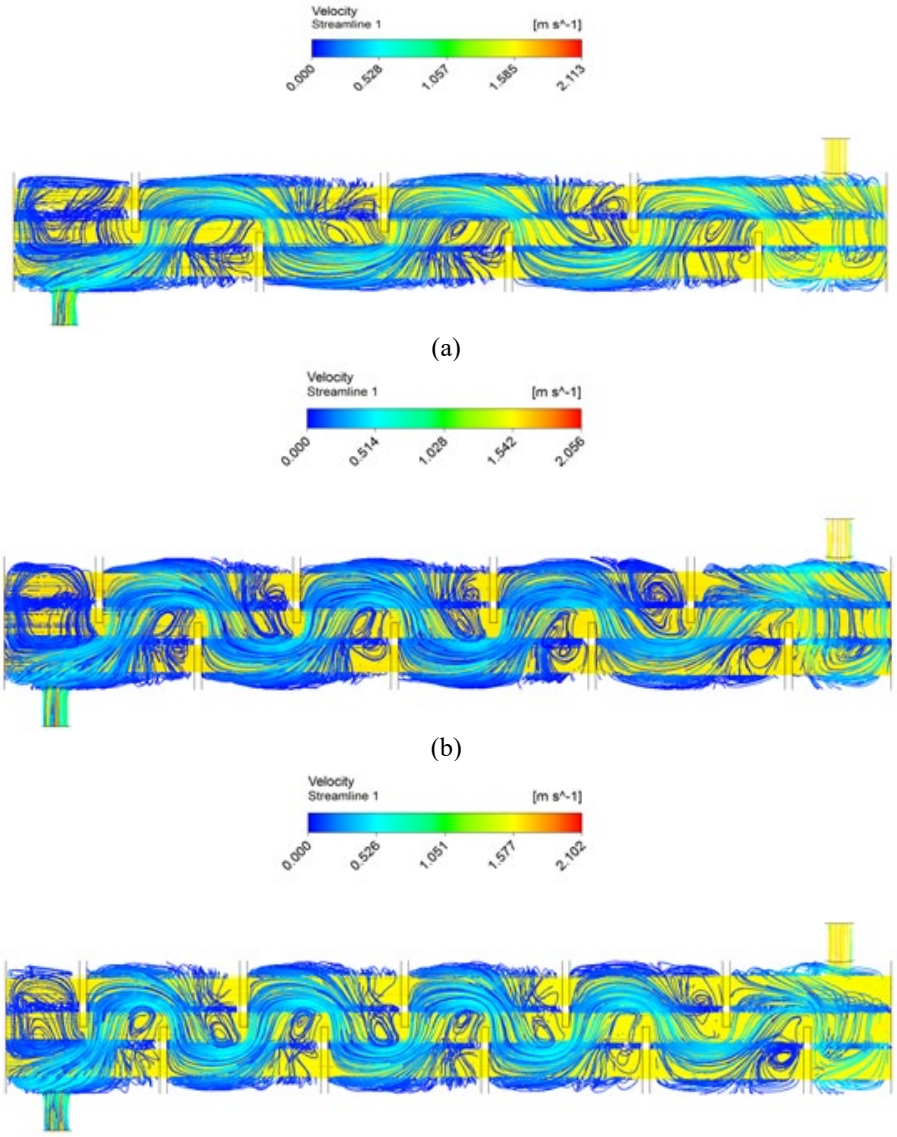

Figure 5. Velocity streamlines for (a) N_b=6, (b) N_b=8, (c) N_b=10, (d) N_b=12 at 0.5 kg/s.

Validation of Results

The foremost aim of this analysis is to validate the findings by comparing the different baffle cuts of STE. The validation could be accomplished by equating the existing literature. In Table 6, a comparison was made by establishing the percentage difference, and the validation is portrayed in the graphs of Figure 6 to Figure 8. Validation of results is carried out on pressure drop, total heat transfer and heat transfer coefficient considering 6, 8, 10 and 12 number of baffles. The graphs illustrated are a comparison of 36% and 50% baffle cut.

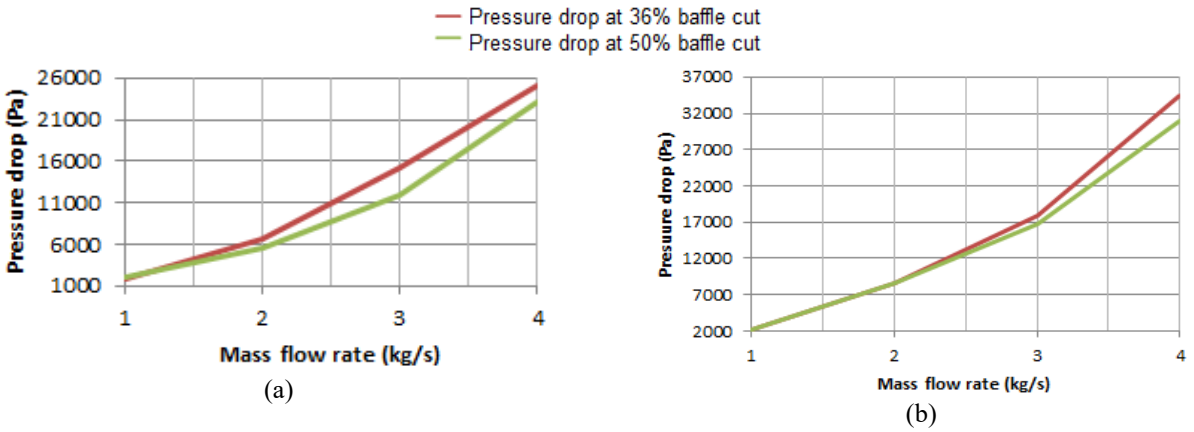

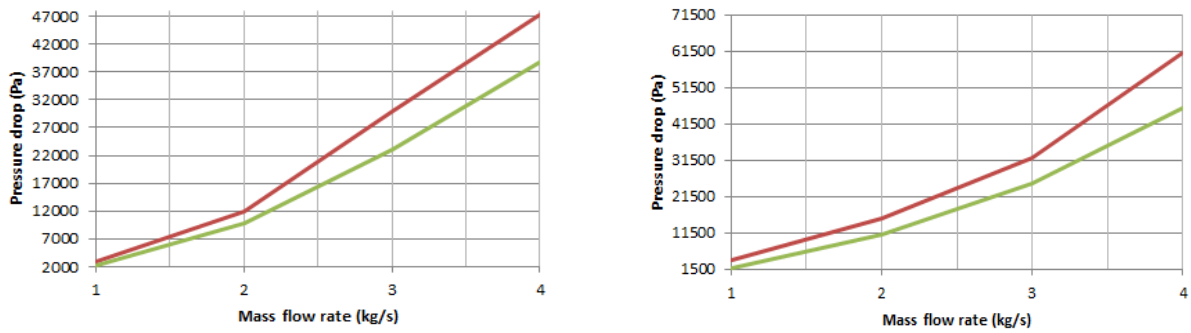

Figure 6. Pressure drop validation for (a) 6 baffles, (b) 8 baffles, (c) 10 baffles and (d) 12 baffles.

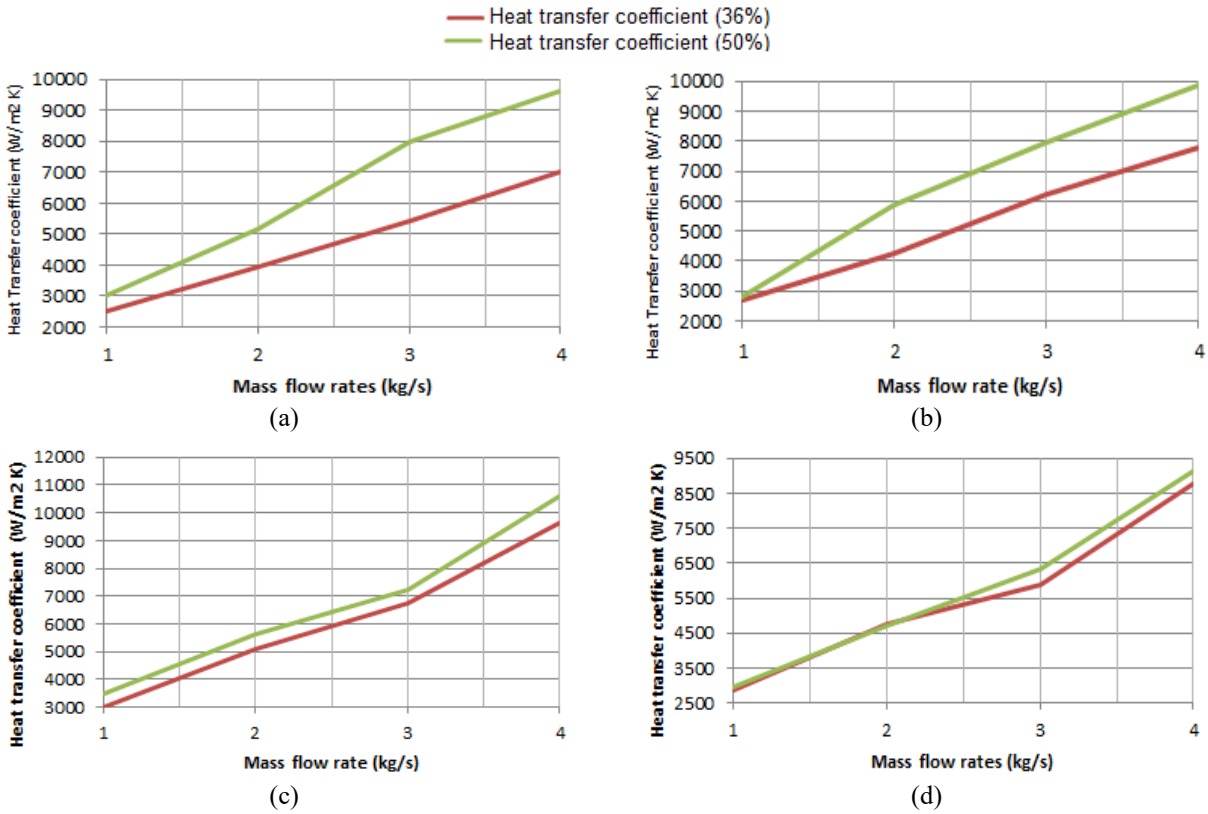

Figure 7. Heat transfer coefficient validation for (a) 6 baffles, (b) 8 baffles, (c) 10 baffles and (d) 12 baffles.

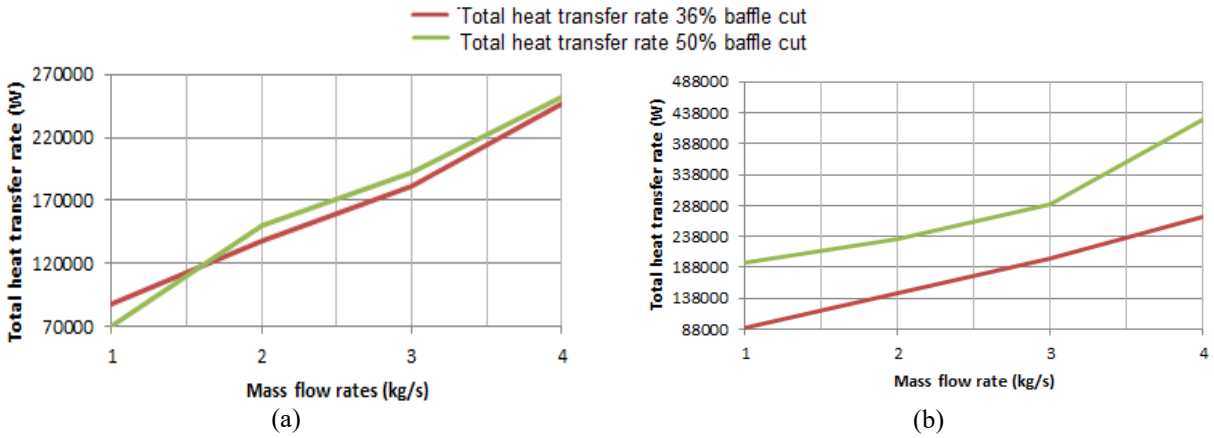

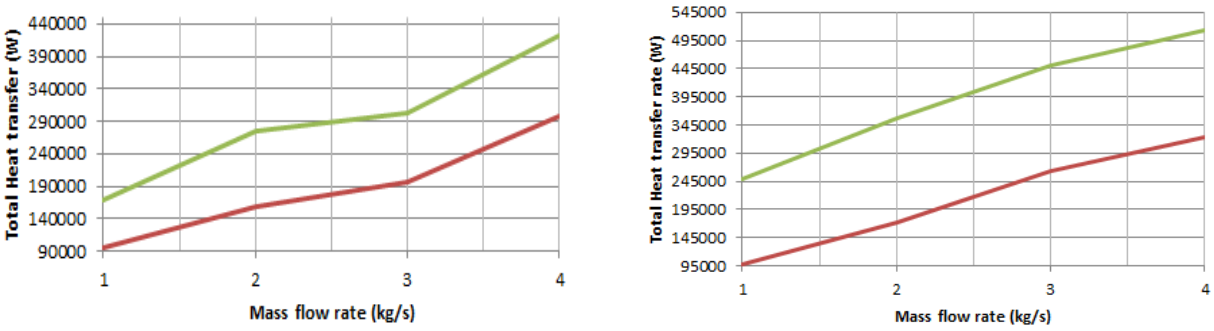

Figure 8. Total heat transfer rate validation for (a) 6 baffles, (b) 8 baffles, (c) 10 baffles and (d) 12 baffles.

CONCLUSION

From the above study, a computational model is used to compute and compare the performance of the shell side of an STE. Shell side performance is resolved by altering the thermal and transport properties as well as the design parameters. The shell side computations are case sensitive to the low-pressure details, so the study is observed using adequate mess density, discretisation, and turbulence modelling. Among three turbulent models k-ε realisable of 1st order discretisation method emerges to be the best one.

Design parameters like baffle spacing from 6 to 12, baffle cut was altered for three different fluid flow rates. The baffle cut has a significant impact on the fluid to fluid heat transfer. The 50% baffle cut gives a better result in contrast with the 36% baffle cut. For this analysis, k-ε std. and k-ε realisable coarse mesh under predicts the outcomes in comparison with the 36% baffle cut. Decreasing the baffle cuts leads to form recirculation zones behind the baffles so that the crossflow windows can not well utilised, which have already been illustrated in Figure 4 to Figure 5 for 12 number of baffles. Hence after increasing the baffle cut and several baffles, such weakness inside the shell is fixed.

For this single segmental baffle design heat exchanger, it was found that the total heat transfer increases for 50% baffle cut with increasing baffle spacing inside the shell. The heat transfer increment is up to 60.66% for 0.5 kg/s mass flow rate, which is higher in comparison with the 36% baffle cut. The pressure drop will increase after flow rate increment; however, in contrast, with a 36% baffle cut, the pressure drop in this study decreases up to a maximum of 44% and a minimum of 1.25%. In future problems like the formation of dead zones, vibrational damage can be overcome by introducing double segmental baffles. Based on this CFD based prediction, a correlation-based approach can be used for better validation of this work.

REFERENCES

[1] Andrews MJ, Master BI. Three-dimensional modeling of a Helixchanger® heat exchanger using CFD. Heat transfer engineering. 2005; 26(6):22-31.

[2] Trp A, Lenic K, Frankovic B. Analysis of the influence of operating conditions and geometric parameters on heat transfer in water-paraffin shell-and-tube latent thermal energy storage unit. Applied Thermal Engineering. 2006; 26(16):1830-9.

[3] Karno A, Ajib S. Effect of tube pitch on heat transfer in shell-and-tube heat exchangers—new simulation software. Heat and mass transfer. 2006; 42(4):263-70.

[4] Jayakumar JS, Mahajani SM, Mandal JC, Vijayan PK, Bhoi R. Experimental and CFD estimation of heat transfer in helically coiled heat exchangers. Chemical engineering research and design. 2008; 86(3):221-32.

[5] Gajapathy R, Velusamy K, Selvaraj P, Chellapandi P, Chetal SC, Sundararajan T. Thermal hydraulic investigations of intermediate heat exchanger in a pool-type fast breeder reactor. Nuclear Engineering and Design. 2008; 238(7):1577-91.

[6] Mohanty S, Arora R, Parkash O. Performance prediction and comparative analysis for a designed, developed, and modeled counterflow heat exchanger using computational fluid dynamics. Computational Thermal Sciences: An International Journal. 2019; 11(5).

[7] Mandal MM, Nigam KD. Experimental study on pressure drop and heat transfer of turbulent flow in tube in tube helical heat exchanger. Industrial and Engineering Chemistry Research. 2009; 48(20):9318-24.

[8] Kharat R, Bhardwaj N, Jha RS. Development of heat transfer coefficient correlation for concentric helical coil heat exchanger. International Journal of Thermal Sciences. 2009; 48(12):2300-8.

[9] Ozden E, Tari I. Shell side CFD analysis of a small shell-and-tube heat exchanger. Energy Conversion and Management. 2010; 51(5):1004-14.

[10] Chen YP, Sheng YJ, Dong C, Wu JF. Numerical simulation on flow field in circumferential overlap trisection helical baffle heat exchanger. Applied Thermal Engineering. 2013; 50(1):1035-43.

[11] Jadhav AD, Koli TA. CFD analysis of shell and tube heat exchanger to study the effect of baffle cut on the pressure drop. International Journal of Research in Aeronautical and Mechanical Engineering. 2014; 2(7):1-7.

[12] Jayakumar JS, Mahajani SM, Mandal JC, Iyer KN, Vijayan PK. Thermal hydraulic characteristics of air–water two-phase flows in helical pipes. chemical engineering research and design. 2010; 88(4):501-12.

[13] Pandey SD, Nema VK. Experimental investigation of heat transfer and friction factor in a corrugated plate heat exchanger. international journal of energy and environment. 2011; 2(2):287-96.

[14] Mandal MM, Serra C, Hoarau Y, Nigam KD. Numerical modeling of polystyrene synthesis in coiled flow inverter. Microfluidics and nanofluidics. 2011; 10(2):415-23.

[15] Moraveji MK, Darabi M, Haddad SM, Davarnejad R. Modeling of convective heat transfer of a nanofluid in the developing region of tube flow with computational fluid dynamics. International communications in heat and mass transfer. 2011; 38(9):1291-5.

[16] Ferng YM, Lin WC, Chieng CC. Numerically investigated effects of different Dean number and pitch size on flow and heat transfer characteristics in a helically coil-tube heat exchanger. Applied Thermal Engineering. 2012; 36:378-85.

[17] Thantharate V, Zodpe DB. Experimental and numerical comparison of heat transfer performance of twisted tube and plain tube heat exchangers. International Journal of Science Engineering and Research. 2013; 4(7):1107-13.

[18] Bhadouriya R, Agrawal A, Prabhu SV. Experimental and numerical study of fluid flow and heat transfer in a twisted square duct. International Journal of Heat and Mass Transfer. 2015; 82:143-58.

[19] Kareem ZS, Jaafar MM, Lazim TM, Abdullah S, Abdulwahid AF. Passive heat transfer enhancement review in corrugation. Experimental Thermal and Fluid Science. 2015; 68:22-38.

[20] Yang J, Liu W. Numerical investigation on a novel shell-and-tube heat exchanger with plate baffles and experimental validation. Energy conversion and management. 2015; 101:689-96.

[21] Pal E, Kumar I, Joshi JB, Maheshwari NK. CFD simulations of shell-side flow in a shell-and-tube type heat exchanger with and without baffles. Chemical engineering science. 2016; 143:314-40.

[22] El Maakoul A, Laknizi A, Saadeddine S, El Metoui M, Zaite A, Meziane M, Abdellah AB. Numerical comparison of shell-side performance for shell and tube heat exchangers with trefoil-hole, helical and segmental baffles. Applied Thermal Engineering. 2016; 109:175-85.

[23] Bichkar P, Dandgaval O, Dalvi P, Godase R, Dey T. Study of shell and tube heat exchanger with the effect of types of baffles. Procedia Manufacturing. 2018; 20:195-200.

[24] Nada SA, Elattar HF, Fouda A, Refaey HA. Numerical investigation of heat transfer in annulus laminar flow of multi tubes-in-tube helical coil. Heat and Mass Transfer. 2018; 54(3):715-26.

[25] Shinde S, Chavan U. Numerical and experimental analysis on shell side thermo-hydraulic performance of shell and tube heat exchanger with continuous helical FRP baffles. Thermal Science and Engineering Progress. 2018; 5:158-71.

[26] Daróczy L, Janiga G, Thévenin D. Systematic analysis of the heat exchanger arrangement problem using multi-objective genetic optimisation. Energy. 2014; 65:364-73.

[27] Das SK, Choi SU, Patel HE. Heat transfer in nanofluids—a review. Heat transfer engineering. 2006; 27(10):3-19.

[28] Standards of Tubular Exchanger Manufacturers Association. Tubular Exchanger Manufacturers Association. Inc., New York. 1959.